Click Here for Full Article

Element fluxes from the volcanic front of Nicaragua and Costa Rica

Michael J. Carr and Ian Saginor

Department of Geological Sciences, Rutgers University, 610 Taylor Road, Piscataway, New Jersey 08854–8066, USA (carr@rutgers.edu)

Guillermo E. Alvarado

Seismology and Volcanology, Instituto Costarricense de Electricidad, Apartado 10032–1000, Costa Rica

Louise L. Bolge

Department of Geological Sciences, Rutgers University, 610 Taylor Road, Piscataway, New Jersey 08854–8066, USA

Now at Department of Earth Sciences, Boston University, 685 Commonwealth Avenue, Boston, Massachusetts 02215, USA

Fara N. Lindsay, Kathy Milidakis, Brent D. Turrin, Mark D. Feigenson, and Carl C. Swisher III

Department of Geological Sciences, Rutgers University, 610 Taylor Road, Piscataway, New Jersey 08854–8066, USA

[1] Geochronologic and geological data define a 600 ka age for the current volcanic front in Costa Rica. In Nicaragua, this age is less constrained but is likely within the range 600 ka to 330 ka. In Costa Rica, the new geochronologic data significantly improve estimates of the volumes of the volcanoes because they define the contact between the active volcanoes and the previous volcanic front, which is substantially older (2.2 to 1.0 Ma). In addition, the contrast in extrusive volcanic flux between western Nicaragua (1.3 × 10^{10} kg/m/Myr) and central Costa Rica (2.4 × 10^{10} kg/m/Myr) is greatly reduced from previous estimates and now within the range of error estimates. We estimate the subducted component of flux for Cs, Rb, Ba, Th, U, K, La, Pb, and Sr by subtracting estimated mantle-derived contributions from the total element flux. An incompatible element-rich OIB source for the Cordillera Central segment in Costa Rica makes the subducted element flux there highly sensitive to small changes in the modeled mantle-derived contribution. For the other three segments studied, the estimated errors in concentrations of highly enriched, subduction-derived elements (Cs, Ba, K, and Pb) are less than 26%. Averaged over the time of the current episode of volcanism, the subduction-derived fluxes of Cs, Ba, K, Pb, and Sr are not significantly different among the four segments of the Central American volcanic front in Nicaragua and Costa Rica. The subduction-derived fluxes of Th and La appear to increase to the SE across Nicaragua and Costa Rica, but the estimated errors in their subduction-derived concentrations are very high, making this variation questionable. The lack of change in the fluxes of Cs, Ba, K, Pb, and Sr argues that the well-defined regional variation in Ba/La is the result of changes in the mode or mechanics of fluid delivery into the mantle wedge, not the total amounts of fluids released from the slab. Concentrated or focused fluids in Nicaragua lead to high degrees of melting. Diffuse fluids in Costa Rica cause lower degrees of melting.

1. Introduction

[2] Although much progress has been made in understanding magma generating processes in the subduction factory beneath arc volcanoes, the goal of calculating a mass balance across a convergent margin has not been satisfactorily reached. The main problem is the considerable difficulty in quantifying the outputs at the forearc, volcanic front and back arc. The largest, most easily measured output is the volcanic front. For Central America, *Patino et al.* [2000] and *Plank et al.* [2002] estimated the flux of subducted incompatible elements out of the volcanic front. However, their age control, a few tephra units dated via marine stratigraphy [e.g., *Ledbetter*, 1985], was inadequate. We present more accurate flux determinations for the volcanic front based on $^{40}Ar/^{39}Ar$ age determinations of lava flows.

[3] Central America (Figure 1) is an excellent place to attempt a mass balance across a convergent margin, especially for elements largely derived from subducted sediment. There are satisfactory physical and geochemical databases for volcanoes [*Carr and Rose*, 1987], maintained at http://www.rci.rutgers.edu/~carr/, and for the Cocos Plate sediment section [*Patino et al.*, 2000]. $^{10}Be/^{9}Be$, an unambiguous tracer of sediment input, reaches its global maximum at Masaya volcano in Nicaragua [*Morris et al.*, 1990], indicating substantial sediment throughput. Several geochemical tracers of subducted sources (e.g., $^{10}Be/^{9}Be$, $^{87}Sr/^{86}Sr$, Ba/La, U/Th) have large and regular geographic variations that allow comparison of regions of high slab signal, western and central Nicaragua, to nearby regions of low slab signal, the Cordillera Central of central Costa Rica [*Carr et al.*, 2003, and references therein]. These areas in close geographic and tectonic proximity share substantial geologic history, yet have very different geochemistry. Sediment sections cored on the Cocos Plate just offshore of Guatemala and Costa Rica are similar, suggesting low variability

in sediment input. Furthermore, from Guatemala to central Costa Rica, there is little sediment accretion [*von Huene and Scholl*, 1991]. However, subduction erosion complicates the input. *Ranero and von Huene* [2000] and *Vannucchi et al.* [2001] present convincing evidence for subduction erosion offshore of central Costa Rica. Smaller amounts of subduction erosion may extend across Nicaragua [*Ranero and von Huene*, 2000].

[4] Geochemical tracers of subduction define a slightly asymmetric chevron along Central America. Ba/La is appropriate for reviewing the regional variation in slab signal (Figure 2a) because it is easily measured and has a strong positive correlation with $^{10}Be/^{9}Be$ [*Leeman et al.*, 1994]. We calculate fluxes for Nicaragua and Costa Rica, where Ba/La ranges from 150 to 15. The high Ba/La values are not surprising because the sediments being subducted are highly enriched in Ba [*Plank and Langmuir*, 1993; *Patino et al.*, 2000]. The subduction of these sediments suggests that changes in the amount of subducted Ba will drive the Ba/La variation. However, Figures 2b and 2c make clear that the regional variation is primarily driven by La, not Ba. Because of this, *Carr et al.* [1990] and *Feigenson and Carr* [1993] developed a flux focusing model for Central America in which tectonic factors, such as slab dip, control the delivery of flux, making it more and less concentrated. Higher concentrations of flux lead to higher degrees of melting. The high Ba concentration in the flux is diluted as the extent of melting increases, resulting in similar Ba concentrations regardless of the degree of melting. La decreases with extent of melting because the La brought in with the flux is not sufficient to counterbalance the diluting effect of higher extent of melting. This model, which links flux concentration and degree of melting, has been substantially modified and improved [e.g., *Reagan et al.*, 1994; *Leeman et al.*, 1994; *Eiler et al.*, 2005] as additional geochemical data and insight have been added. *Carr et al.* [1990] and *Feigenson and Carr* [1993] implicitly
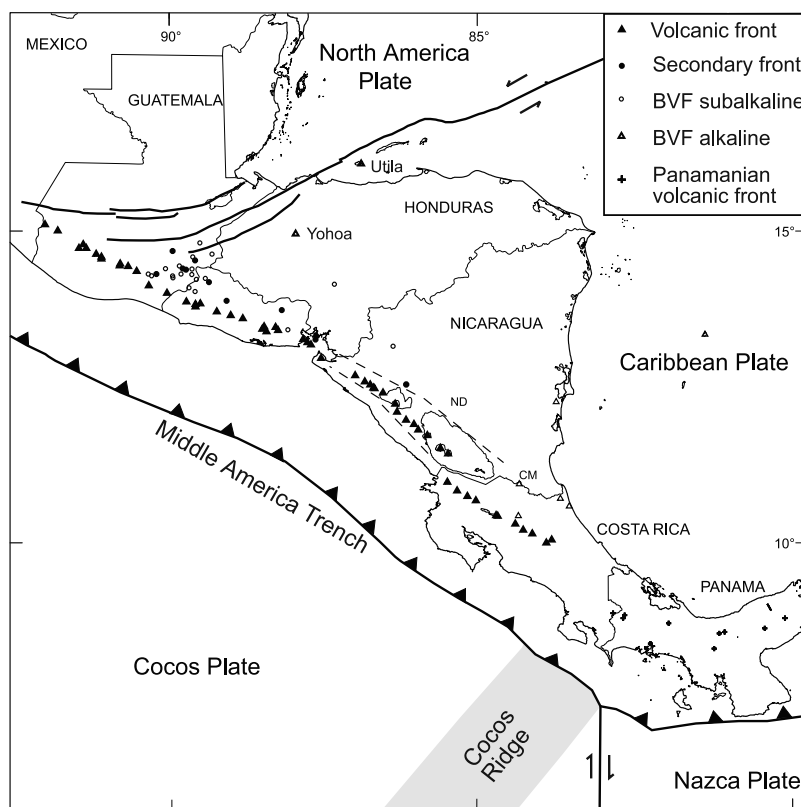
Figure 1. Location map for Central American volcanoes. CM marks the location of Cerro Mercedes. Dashed lines mark position of Nicaraguan Depression (ND).

assumed a constant flux across the region but this is a soft assumption, not required by the geochemistry. The goal of the current work is to determine whether or not the absolute amount of flux of highly incompatible elements varies between Nicaragua and Costa Rica. In other words, is the peak in Nicaragua the result of a higher amount of flux, a stronger focusing of a constant flux or some combination of the two?

[5] There are substantial difficulties in making estimates of element fluxes. On the geochemical side, the major problem is the demonstrated complexity of sources. The sub-arc mantle beneath central Costa Rica includes an enriched ocean island basalt (OIB) component [*Malavassi*, 1991; *Leeman et al.*, 1994; *Herrstrom et al.*, 1995; *Feigenson et al.*, 2004]. The source of this OIB input is poorly constrained and could have originated in the mantle wedge or the subducted plate. *Feigenson et al.* [2004] reviewed this problem and found that few of the several hypotheses concerning this issue can be ruled out. Outside of central Costa Rica, REE inverse modeling suggests that the mantle may consist of at least two compo-

nents, a MORB source and a less depleted source [*Feigenson and Carr*, 1993]. The subducted oceanic crustal section adds additional complexity. An East Pacific Rise MORB crust is subducting outboard of Nicaragua and northwestern Costa Rica and a Cocos-Nazca Ridge MORB crust with Galapagos derived seamounts is subducting outboard of central Costa Rica [e.g., *von Huene et al.*, 2000]. The sedimentary stratigraphy includes two units with large differences in geochemistry [*Patino et al.*, 2000], a basal carbonate section of roughly 200 m and an upper hemipelagic section of roughly 200 m. Recently, *Eiler et al.* [2005] defined plausible depleted mantle (DM) and OIB mantle compositions and identified two separate slab-derived fluxes, one with low $\delta^{18}O$ and one with high $\delta^{18}O$. The former is most likely a hydrous fluid with a strong contribution from the subducted Cocos mantle and the latter is most likely a melt of the subducted sediment.

[6] The mass flux at the volcanic front consists of the existing volcanic edifices, distal tephras, earlier volcanic units, sediments derived by erosion, and a wide range of intrusives including mafic cumu-
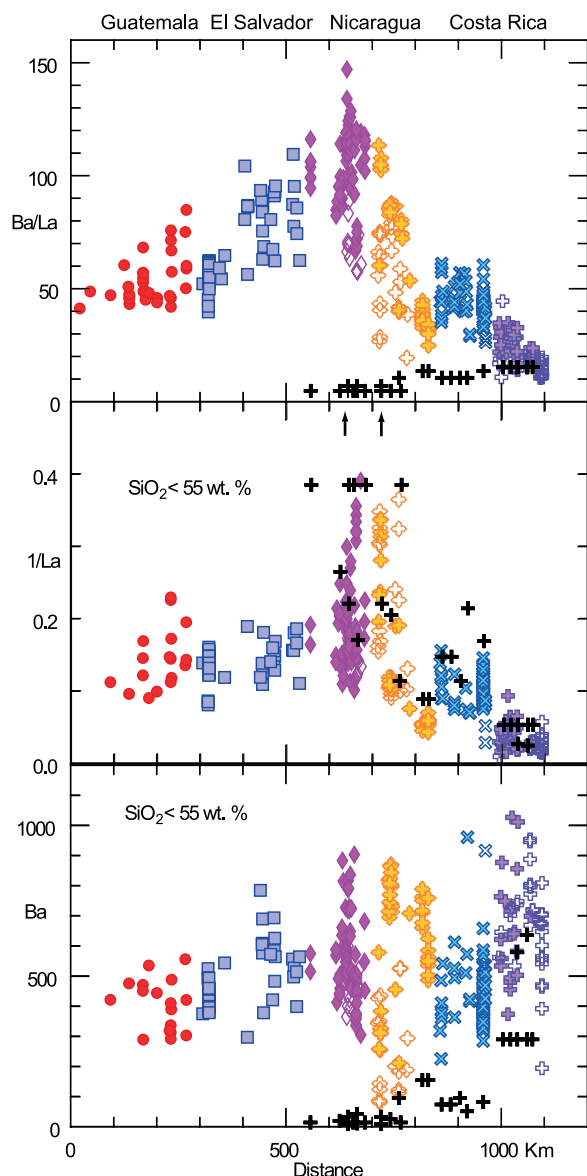
Figure 2. Subduction signal, Ba/La, and its two components along the volcanic front. Symbols mark segments defined primarily by right stepping jogs in the volcanic front. Filled symbols are the volcanics with HFSE depletions. Open symbols are the HFSE-rich suites in Nicaragua and Costa Rica. Black symbols and arrows are estimated mantle contributions.

lates, which are likely near the Moho [e.g., *Herzberg et al.*, 1983], gabbroic to granitic bodies within the crust, and shallow dikes. Obtaining a flux requires defining a volume of igneous output and identifying the time interval over which it was produced. A bottom-up or long-term approach can be achieved in an island arc by measuring the total volume of arc-derived crust and determining the

onset of arc–related igneous activity. However, pauses in magmatic activity may generate a long-term rate that is inappropriate for magmatically active periods. We apply a top-down or short-term approach here, by focusing on volcanic output that can be quantified from geologic mapping of lavas and tephras. This restricted approach captures a fair snapshot of the ongoing magmatic process. However, it does not measure total magmatic output because intrusives and eroded materials are not included. Our top-down approach provides a partial extrusive volcanic flux because we have not yet determined appropriate erosion rates.

[7] To provide more accurate estimates of extrusive volcanic fluxes, we report new $^{40}Ar/^{39}Ar$ ages on lava and pyroclastic flows that geologic mapping and geomorphic expression indicate are critical for understanding the rate of cone construction in Costa Rica and Nicaragua. Our results add to a growing body of geochronological data. *Ehrenborg* [1996] and *Plank et al.* [2002] recently summarized and added to the previous geochronological work in Nicaragua. *Alvarado et al.* [1992] summarized the geochronology of Costa Rican volcanics and *Gillot et al.* [1994] provided several new K-Ar ages and estimates of the volume of the major volcanic units. *Vogel et al.* [2004] and *Pérez et al.* [2006] defined the age framework of several Costa Rican ignimbrite sheets. A substantial number of new $^{40}Ar/^{39}Ar$ ages allowed *Gans et al.* [2002, 2003] to propose that a series of discrete volcanic episodes has constructed the volcanic provinces of Costa Rica.

2. Data

2.1. $^{40}Ar/^{39}Ar$ Age Determinations

[8] Table 1 provides new ages on 45 samples from Nicaragua and Costa Rica. The sample preparation and data analysis procedures used, as well as a table providing the results of the individual step heating experiments, are in auxiliary material Text S1.[1] A typical example of a $^{40}Ar/^{39}Ar$ age determination is provided in Figure 3.

2.2. Volumes of Volcanic Edifices

[9] The volume of each volcanic center was calculated using digitized areas within 100 m contour intervals on topographic maps. Many volcanoes

Table 1. Age Determinations for Volcanic Rocks From Nicaragua and Costa Rica[a]

Sample ID	Lat.	Lon.	Material	Plateau Age, ka	Integrated Age, ka	Isochron Age, ka	$^{40}Ar/^{36}Ar$ Intercept	MSWD	^{39}Ar on Plateau	Note[b]	Volcano
					Nicaragua						
SJ-3	12.319	−85.985	matrix	no plateau	6800 ± 70	7110 ± 60	287 ± 5	3.0	88%		San Jacinto
LL-4	12.385	−85.874	matrix	9480 ± 30	8740 ± 50	9540 ± 70	281 ± 6	3.3	66%		Las Lajas
C-51	12.742	−87.249	matrix	3500 ± 30	3440 ± 40	3550 ± 50	294 ± 0.6	1.0	94%		unnamed
C-51	"	"	matrix	3590 ± 30	3550 ± 40	3640 ± 50	294 ± 0.8	1.0	98%		"
LN-6	12.680	−86.601	matrix	1130 ± 50	1060 ± 40	1560 ± 150	286 ± 1.9	1.0	80%		"
LN-7	12.684	−86.609	matrix	1480 ± 20	1470 ± 40	1480 ± 60	295 ± 1.9	2.0	97%		"
NIC-SC-2000-1	12.602	−87.047	matrix	160 ± 60	320 ± 120	190 ± 70	299.3 ± 1.3	1.2	77%		San Cristóbal
NIC-TE-111	12.619	−86.887	matrix	330 ± 20	400 ± 30	300 ± 30	303 ± 3	1.3	76%		Telica
NIC-TE-114	12.618	−86.889	matrix	172 ± 16	170 ± 30	260 ± 70	292 ± 3	0.3	100%		"
NIC-TE-120	12.639	−86.766	matrix	173 ± 11	150 ± 20	215 ± 19	293.1 ± 1	0.5	100%		"
NIC-LP-106	12.514	−86.631	matrix	65 ± 11	150 ± 40	17 ± 6	301.9 ± 1.8	4.3	79%		Las Pilas
NIC-MT-2000-2	12.478	−86.607	matrix	71 ± 9	100 ± 15	20 ± 6	305 ± 3	4.9	57%		Momotombo
NIC-MT-2000-6	12.387	−86.525	matrix	283 ± 12	290 ± 20	290 ± 20	295 ± 2	0.6	100%		"
NIC-MT-2000-6	"	"	matrix	280 ± 20	280 ± 30	280 ± 30	295 ± 2	0.9	100%		"
NIC-M-10	11.485	−85.493	matrix	76 ± 6	87 ± 7	52 ± 16	301 ± 5	3.0	78%		Maderas
					Costa Rica						
CR-RV-201	10.787	−85.259	matrix	380 ± 20	360 ± 40	290 ± 70	295.2 ± 1.4	1.3	99%		Rincón
CR-RV-04-12	10.769	−85.278	matrix	564 ± 5	555 ± 7	557 ± 8	300 ± 4	1.4	76%		"
CR-RV-02-62	10.780	−85.421	matrix	1138 ± 30	1258 ± 60	1,238 ± 50	284 ± 5	1.7	76%		pre-Rincón
CR-RV-02-66	10.815	−85.416	matrix	1611 ± 200	1611 ± 600	906 ± 500	307 ± 13	0.3	98%		"
CR-RV-04-13	10.730	−85.392	matrix	2176 ± 19	2144 ± 14	2179 ± 14	294.2 ± 1.3	2.5	91%		"
CR-MV-02-40	10.852	−85.148	matrix	5654 ± 30	5356 ± 30	5537 ± 170	320 ± 70	15.0	56%	2	pre-Miravalles
CR-MV-04-9	10.716	−85.175	matrix	75 ± 4	116 ± 4	68 ± 7	301.2 ± 1.5	2.7	66%		Miravalles
CR-MV-04-11	10.681	−85.145	matrix	548 ± 11	560 ± 20	580 ± 70	294 ± 70	3.5	88%		"
CR-TE-02-38	10.596	−85.049	matrix	1913 ± 20	1681 ± 60	2174 ± 40	221 ± 9	1.2	90%		pre-Tenorio
CR-TE-04-5	10.596	−85.029	matrix	740 ± 30	743 ± 18	740 ± 16	287 ± 4	2.7	75%		"
CR-TE-02-31	10.710	−84.980	matrix	95 ± 8	70 ± 20	124 ± 14	291.7 ± 1.3	1.5	75%		Tenorio
CR-TE-02-32	10.785	−84.955	matrix	372 ± 30	513 ± 80	209 ± 40	330 ± 10	0.2	94%	1	"
CR-TE-04-6	10.609	−85.039	matrix	548 ± 6	543 ± 8	550 ± 8	294 ± 2	1.3	94%		"
CR-TE-04-7	10.614	−85.043	matrix	90 ± 4	102 ± 6	81 ± 5	303 ± 3	1.1	90%		"
CR-TE-04-8a	10.623	−85.049	matrix	266 ± 19	280 ± 20	270 ± 30	309 ± 13	1.5	61%		"
CR-TE-04-8b	10.623	−85.049	matrix	371 ± 12	368 ± 16	390 ± 30	294 ± 3	0.5	100%		"
CR-PO-02-22	10.341	−84.446	matrix	252 ± 30	232 ± 100	312 ± 70	290 ± 6	0.4	100%		Platanar
CR-PP-02-26	10.280	−84.264	wr	No plateau	2380 ± 170	440 ± 40	325.4 ± 1.7	5.1		3	"
CR-PP-02-27	10.284	−84.263	matrix	554 ± 20	705 ± 50	352 ± 40	315 ± 3	2.3	76%	1	"
CR-PO-02-28	10.363	−84.236	wr, plg	260 ± 18	302 ± 40	201 ± 30	301 ± 2	2.3	67%		Poás
CR-PO-02-29	10.351	−84.221	wr, plg	293 ± 18	383 ± 40	201 ± 30	305 ± 3	1.5	76%		"
CR-B-02-8	10.324	−84.167	matrix	238 ± 6	224 ± 11	262 ± 10	289.6 ± 1.7	0.3	74%		Barva

Table 1. (continued)

Sample ID	Lat.	Lon.	Material	Plateau Age, ka	Integrated Age, ka	Isochron Age, ka	$^{40}Ar/^{36}Ar$ Intercept	MSWD	^{39}Ar on Plateau	Note[b]	Volcano
CR-B-02-9	10.320	−84.156	matrix	**201 ± 20**	201 ± 30	282 ± 50	286 ± 5	0.7	93%		"
CR-B-02-15	10.400	−84.081	matrix	**259 ± 9**	221 ± 50	272 ± 12	294.0 ± 0.7	1.5	95%		"
CR-B-02-16	10.408	−84.076	matrix	335 ± 7	386 ± 19	**246 ± 17**	321 ± 4	0.2	93%	1	"
CR-IZ-02-1	9.891	−83.855	matrix	8 ± 7	26 ± 15	**57 ± 13**	287 ± 2	1.3	50%		Irazú
CR-IZ-02-2	9.899	−83.835	matrix	**20 ± 12**	7 ± 19	9 ± 3	289 ± 3	0.8	54%		"
CR-IZ-02-5	9.884	−83.751	matrix	**598 ± 16**	584 ± 50	602 ± 20	293 ± 7	1.9	94%		"
CR-IZ-02-19	9.952	−83.929	biotite	**137 ± 5**	135 ± 10	147 ± 10	293 ± 2	1.1	99%		"
CR-IZ-02-20	9.987	−83.943	matrix	544 ± 3	516 ± 6	**573 ± 6**	269 ± 4	0.7	88%		"
CR-IZ-02-17	9.862	−83.795	biotite	**861 ± 6**	856 ± 8	872 ± 9	292 ± 3	1.2	100%		San Jeronimo
CR-IZ-02-17	"	"	"	**868 ± 9**	868 ± 10	843 ± 16	304 ± 8	1.1	98%		"
CR-IZ-02-17	"	"	plag	830 ± 8	819 ± 9	**853 ± 11**	284 ± 3	0.6	96%		"

[a] Preferred ages in bold.
[b] Notes: 1, Saddle Shaped spectra; 2, three step plateau, first two steps not used in isochron; 3, no plateau, no reliable age, meets none of the reliability criteria.

have irregular bases that required adding in wedge or slab like volumes. Some volcanoes have produced ashflow sheets that extend beyond the current topographic limits of the volcanic edifice. All of the ashflow units with ages of 600 ka or less and whose volumes have been determined have been included in the volumes. The Alto Palomo tephra near Platanar volcano in Costa Rica [*Villegas*, 2004; *Vogel et al.*, 2004] has an appropriate age but lacks a well-determined volume and was not included. The ashflow sheets near Malpaisillo, Nicaragua are not included in any volume because the source, the Malpaisillo Caldera, proposed by *van Wyk De Vries* [1993], has not been proven and the age is thought to be late Tertiary. Table 2 lists the calculated volumes and the raw data are in auxiliary material Text S2.

[10] Volumes critically depend on the determination of the pre-volcanic base which relies heavily on geologic understanding. For example, *Stoiber and Carr* [1973] estimated a volume of only 11 km³ for Masaya volcano, based on the size of the most recent caldera. Subsequently, *van Wyk de Vries* [1993] recognized that the Masaya caldera was part of a large ignimbrite shield with a volume of over 200 km³, the Masaya/Las Sierras volcanic center. We are currently trying to obtain reliable ages for large ignimbrites at the base of the Las Sierras. The current volume assumes an age of less than 600 ka for the entire complex, which may well be wrong. These changes in the volume of Masaya are the result of improved geologic understanding, not fluctuations from random error.

2.3. Trace Element Analysis

[11] Many previously published geochemical data for Central America [e.g., *Patino et al.*, 2000] were re-determined after powdering the samples in alumina containers. These samples, collected from 1972–1990, were originally powdered in tungsten carbide vessels, rendering their Nb and Ta analyses suspect or completely misleading. HR-ICP-MS trace element analyses, used here, follow the procedures of *Bolge et al.* [2006].

3. Results

[12] We determine an extrusive volcanic flux by measuring the volumes of volcanic centers (Table 2) and determining the start of the current episode of volcanism. The $^{40}Ar/^{39}Ar$ ages in Table 1 with additional $^{40}Ar/^{39}Ar$ ages from *Vogel et al.* [2004] indicate a well-defined pulse of volcanic
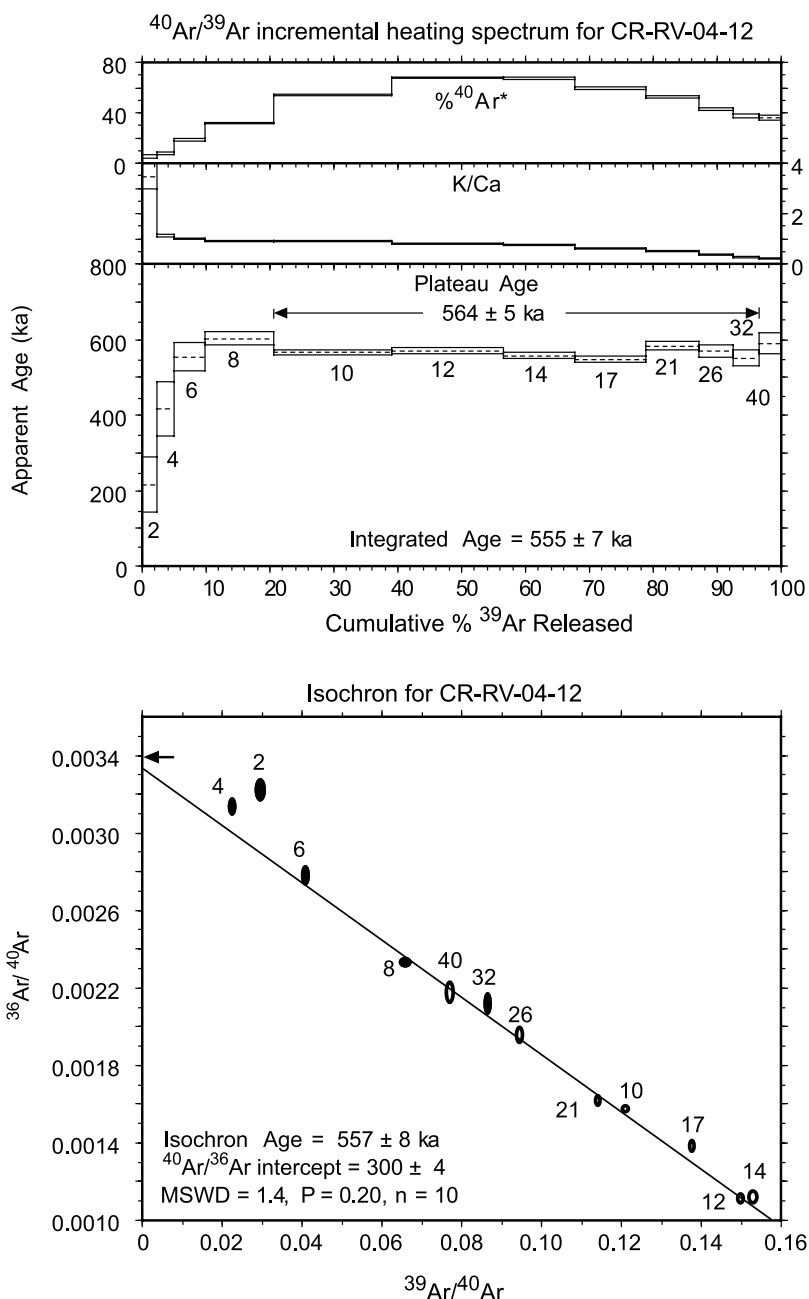
Figure 3. Step heating spectra for sample CR-RV-04-12 from Rincón de la Vieja volcano. The heating steps, in watts, are written below Ar release steps in the plateau diagram and adjacent to the error ellipses in the inverse isochron diagram. Steps 2 and 4 watts not included in isochron.

activity in Costa Rica beginning at about 600 ka (Figure 4) and continuing to the present. In Nicaragua, the start of the current episode of volcanism is not well determined.

[13] We estimate element flux by multiplying the extrusive volcanic flux by the subduction-derived component of the average lava. The subduction component is the difference between the mean lava composition and an estimated melt composition generated from a flux-free mantle wedge. To estimate the contribution from the mantle wedge, we use, with minor modification, the melt model, mineral mode and partition coefficients of *Eiler et al.* [2005]. Because of the unusual geochemistry of Cordillera Central lavas, *Eiler et al.* [2005] estimated an enriched or OIB source for Central American magmas. Oxygen isotope constraints allowed *Eiler et al.* [2005] to invert lava composi-

Table 2. Mass Fluxes for Nicaragua and Costa Rica

Volcanic Center (Subgroup)	Fraction of Volume	Volume,[a] km³	Length, km	Age, Ma	Volume Flux, km³/km/Myr	Mass Flux,[b] 10^{10} kg/m/Myr
Cosigüina	1.00	57	-	-	-	0.29
San Cristóbal	1.00	109	-	-	-	0.56
Telica (high U/La)	0.43	12	-	-	-	0.06
Telica (high Ba/Th)	0.43	12	-	-	-	0.06
Telica (HFSE-rich)	0.14	4	-	-	-	0.02
Rota	1.00	7	-	-	-	0.04
Las Pilas-Cerro Negro	0.82	23	-	-	-	0.12
Las Pilas (HFSE-rich)	0.18	5	-	-	-	0.03
Momotombo	1.00	17	-	-	-	0.09
Apoyeque	1.00	12	-	-	-	0.06
Western Nicaragua totals		259	166	0.33	4.7	1.32
Error estimate in %		15	5	40	43	43
Nejapa	0.75	2	-	-	-	0.01
Nejapa (HFSE-rich)	0.25	1	-	-	-	0.00
Masaya-Las Sierras-Apoyo	1.00	203	-	-	-	1.04
Mombacho	0.95	34	-	-	-	0.17
Granada (HFSE-rich)	0.05	2	-	-	-	0.01
Zapatera	1.00	9	-	-	-	0.05
Concepción	1.00	31	-	-	-	0.16
Maderas	1.00	30	-	-	-	0.15
Eastern Nicaragua totals		312	137	0.33	6.9	1.59
Error estimate in %		30	5	40	50	50
Orosí	1.00	76	-	-	-	0.39
Rincón de la Vieja	1.00	102	-	-	-	0.52
Miravalles	1.00	62	-	-	-	0.31
Tenorio	1.00	53	-	-	-	0.27
Guanacaste totals		293	92	0.60	5.3	1.49
Error estimate in %		20	10	10	24	24
Arenal	1.00	11	-	-	-	0.03
Platanar	1.00	84	-	-	-	0.26
Poás	1.00	97	-	-	-	0.30
Barba	0.50	99	-	-	-	0.31
Barba (HFSE-rich)	0.50	99	-	-	-	0.31
Irazú-Sapper	0.50	130	-	-	-	0.40
Irazú-Haya (HFSE-rich)	0.50	130	-	-	-	0.40
Turrialba	1.00	112	-	-	-	0.35
Cordillera Central totals		761	150	0.60	8.5	2.37
Error estimate in %		25	15	10	31	31

[a] Total volumes for each center with subgroups can be obtained by summing the groups.
[b] Density assumed to be 2800 kg/m³. Length and age factors of flux taken from segment totals.

tions to obtain the compositions of two fluid fluxes from the slab as well as the degree of melting and the proportions of the four sources; DM, OIB, low-$\delta^{18}O$ fluid and high-$\delta^{18}O$ fluid. Our modeling is much simpler, we use two mantle wedge sources, DM and OIB to match the compositions of Nb, Ta and the HREEs. We derive different compositions for DM and OIB (Figure 9), but obtain similar proportions of the mantle wedge sources and similar degrees of melting (Table 4).

3.1. Extrusive Volcanic Flux for Costa Rica

[14] In Costa Rica, a rich background of geochronologic work [*Alvarado et al.*, 1992; *Gillot et al.*,

1994; *Gans et al.*, 2003; *Vogel et al.*, 2004] and geologic mapping [*Tournon and Alvarado*, 1997] guided our sampling, allowing us to select critical areas not addressed by previous work. The extensive geochronologic survey of the Costa Rican volcanic belt by *Gans et al.* [2003] suggested several post-Miocene peaks of volcanic activity separated by apparent lulls: with peaks at 6–4 Ma, 2–1 Ma, 600–400 ka and 100–0 ka. We designed our sampling to better define the boundaries between these age peaks, especially the contact mapped by *Tournon and Alvarado* [1997] between the 2–1 Ma volcanics and the volcanics younger than 600 ka. The 2–1 Ma volcanics will be referred to here as the Monteverde volcanic
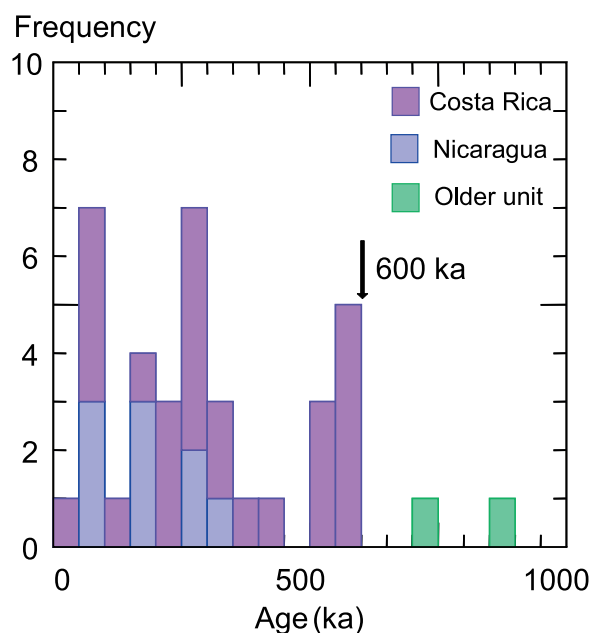
Figure 4. Histogram of $^{40}Ar/^{39}Ar$ ages for Costa Rican and Nicaraguan volcanics.

front (VF) and the 600 ka and younger volcanics will be referred to as the active VF.

[15] Since the 1997 map of *Tournon and Alvarado* [1997], geochronologic work and mapping by G. E. Alvarado and co-workers from the Central American School of Geology at the University of Costa Rica have increased the extent of the Monteverde VF at the expense of the active volcanoes. Figure 5 sketches the currently recognized boundaries and shows that the active volcanoes primarily occur in two major ranges, the Cordillera de Guanacaste

and the Cordillera Central. In the Cordillera de Guanacaste, our $^{40}Ar/^{39}Ar$ results aided this mapping by obtaining ages for flows on either side of the contact. Four samples (with ages of 1.13 Ma, 1.60 Ma, 2.16 Ma and 2.18 Ma) better define the Monteverde VF and slightly extend its range to 2.2 Ma. At Rincón de la Vieja volcano we obtained an age of 564 ka on a flank lava selected for its high degree of erosion. Similarly, at Miravalles and Tenorio volcanoes we obtained ages of 548 (coincidentally equal) on eroded flow fields from the lower flanks. These data verify the presence of the 600–400 ka peak in the Guanacaste region. Because the contact between the active VF and the Monteverde VF can be mapped throughout the Guanacaste segment, we estimate a small error in volume (20%).

[16] In the Cordillera Central, the recognition of older volcanics and sediments at roughly 1500 m elevations throughout the Cordillera decreases the estimated volumes of these volcanic centers. The basal lavas at Irazú in the valley of the Rio Reventazón outcrop at 1500 m. Miocene sediments and Pliocene lavas comprise the lower SE flank of Turrialba volcano with uppermost outcrops that just reach the 1500 contour. At Barva volcano recent fieldwork uncovered sediments on the SE flank that extend from 700 to 1500 m. At Platanar volcano, older volcanics crop out on the SW flank at elevations as high as 2000 m. Therefore the active volcanoes (600 ka and younger volcanics) of the Cordillera Central nearly obscure an older volcanic and sedimentary massif that extends the length of the Cordillera and has a summit elevation of roughly 1500 m.
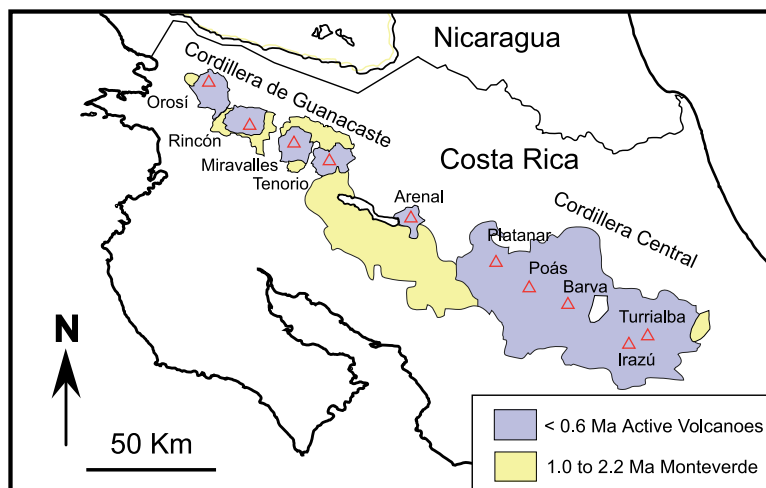

Figure 5. Map of active volcanic front and Monteverde volcanic front in Costa Rica.

[17] Volumes estimated for the Cordillera Central have two components; the larger component (75%) includes all the topography above 1500 m and the smaller component comes from the NE side of the Cordillera, where young volcanics outcrop as low as 300 m. Field work indicates that these flank lavas and tephras are a thin cover on a buried massif of older volcanics and sediments. We estimated volumes of this cover using a thickness of 100 m for the lower flank (elevations below 1000 m) and a thickness of 200 m for the upper flank (elevations between 1500 and 1000 m). These flank veneers comprise 25% of the total volume of the active volcanoes of the Cordillera Central and we use that percentage as the error estimate for the Cordillera Central volumes.

[18] We sought to define a boundary separating the 600–400 ka and 100–0 ka peaks proposed by *Gans et al.* [2003]. However, we obtained nine new ages between 400 ka and 100 ka. Therefore we doubt there was a pause in extrusive volcanic activity between 400 ka and 100 ka. Geomorphological differences, apparent on topographic maps and satellite images, suggest pauses at individual volcanoes, but the new ages indicate that such pauses are local, not segment wide. In contrast, we were successful in using geomorphology to locate the oldest flows; six samples yielded ages between 548 and 598 ka. We agree with *Gans et al.* [2003] that a substantial outpouring of lava began about 600 ka.

[19] Two of our Costa Rican samples have ages in the lull between the Monteverde VF and 600 ka. One, a lava from Tenorio volcano, has an age of 740 ka. The other is the San Jerónimo ash flow tuff with an age of 855 ka. We sampled this welded tuff because geologic mapping [*Krushensky*, 1972; *Alvarado et al.*, 2006] places it beneath the basaltic and andesitic lavas that comprise the lower flanks of Irazú volcano. These two ages clearly show that volcanism did not entirely cease between 1 Ma and 600 ka.

[20] The two major volcanic ranges, the Cordillera de Guanacaste and the Cordillera Central (Figure 5) are separated by a volcanic gap of 80 km that is interrupted only by the small Arenal volcanic center. This gap was not present as recently as 1 Myr ago [*Gillot et al.*, 1994]. The location of the Monteverde volcanic front is similar to that of the present volcanic front in the Cordillera de Guanacaste and the Cordillera Central, but profoundly different in the intervening region. In the area of the gap, pierced only by the small Arenal volcanic

center, the Monteverde VF makes a large ridge whose axis is about 15 km trenchward of Arenal. The cessation of activity in the area between the Cordillera de Guanacaste and the Cordillera Central marks a substantial change in the Costa Rican volcanic front after about 1 Ma. Furthermore, when volcanism resumed near Arenal about 100 ka ago [*Gillot et al.*, 1994], it was located 10 to 15 km NE of its former axis.

[21] Our new $^{40}Ar/^{39}Ar$ ages confirm the proposed peak in volcanic activity starting at about 600 ka. With the exception of Arenal, the Costa Rican volcanic centers all have lava fields in the 600–500 ka age range [*Gans et al.*, 2003, *Gillot et al.*, 1994; *Alvarado et al.*, 1992; this work]. The peak, starting at 600 ka, followed a reorganization of the volcanic front; specifically, the near cessation of volcanism and the repositioning of the volcanic front in the 80 km region, centered on Arenal. These two factors lead us to use 600 ka as the datum for estimating an extrusive volcanic flux for Costa Rica.

3.2. Extrusive Volcanic Flux for Nicaragua

[22] *Patino et al.* [2000] estimated ages for several segments of the volcanic front in Central America, primarily using the ages of large pyroclastic deposits assumed to predate all the active volcanoes. The Nicaraguan estimate (135 ka) was based on the J1 tephra [*Ledbetter*, 1985] whose distinctly high FeO content makes the Masaya-Las Sierras complex the likely source [*Walker et al.*, 1993]. Toward the Pacific coast from Masaya volcano, the initial volcanic deposits, which rest on Plio-Pleistocene marine sediments, are thick andesitic to dacitic pyroclastic flows. The J1 tephra was assumed to be a fall deposit associated with these flows and the entire Nicaraguan volcanic front was assumed to be younger than the J1 tephra. This obviously weak chain of assumptions was a primary motivation for our current work.

[23] The Nicaraguan volcanic front is roughly parallel to and within the Nicaraguan Depression (Figures 1 and 6). The major Nicaraguan lakes and the Gulf of Fonseca, separating Nicaragua from Honduras and El Salvador, also lie within the Depression, suggesting active subsidence. However, most shallow earthquakes occur along the volcanic axis, rather than along either the NE or SW side of the Depression. The flat topography of the Depression simplifies measurement of the volumes of volcanoes. However, alluvial and lacustrine sedimentation has buried the earliest lavas of the active
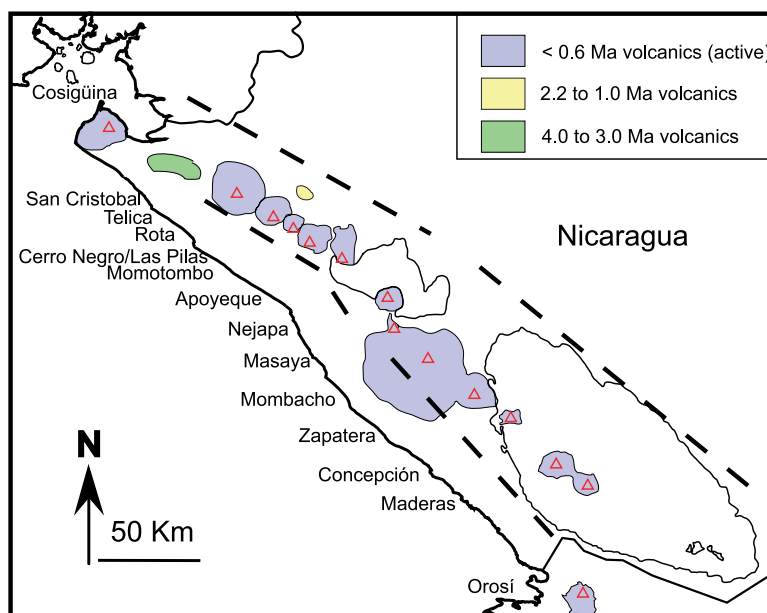
Figure 6. Map of post-Miocene volcanics in Nicaragua. Dashed lines are borders of Nicaraguan Depression.

volcanoes, making it difficult to determine a time of onset. Because the flanks of the Nicaraguan volcanoes, with the exception of SW side of the Masaya volcanic center, merge into alluvial and lacustrine sediments and tephra deposits, the contact between the earliest lavas of the active volcanoes and the previous generation of volcanic deposits is not exposed. Therefore additional assumptions are needed to calculate rates of extrusive volcanic flux.

[24] Our new $^{40}Ar/^{39}Ar$ ages for Nicaraguan lavas and tephra fall into four groups. Two samples, with ages of 9.5 Ma and 7.1 Ma, are from the NE border of the Nicaraguan Depression and within the 7–9 Ma age band of *Plank et al.* [2002]. One sample, with an age of 3.5 Ma, is from an eroded volcanic terrain outcropping along the volcanic front between San Cristóbal and Cosigüina volcanoes (Figure 6). Two samples with ages of 1.13 and 1.48 Ma are from partially buried volcanic remnants located between the Miocene volcanics on the NE border of the Nicaraguan Depression and the active volcanic front (Figure 6). These ages are within the range of the Monteverde VF in Costa Rica. The remaining eight samples are lavas collected from the most eroded sectors of the active volcanoes. Topographic maps and satellite images reveal few highly dissected areas that are likely to expose old lavas. Figure 7 shows the ages obtained from the highly dissected sector of Telica volcano. The eroded area between the three samples was

more altered than the flanks and did not yield a reliable age. The $^{40}Ar/^{39}Ar$ ages we obtained from the oldest available sectors of the active volcanoes range from 65 to 330 ka. The oldest lava sampled is slightly more than half as old as the 600 ka datum we determined for Costa Rica.

[25] The existing age data for Nicaragua are consistent with the volcanic history of Costa Rica during the last 2.2 million years. Just NE of the current volcanic axis are two Nicaraguan samples with ages of 1.13 and 1.48 Ma, within to 2.2 to 1.0 Ma age extent of the Monteverde VF. The Nicaraguan ages younger than 1.0 Ma (Figure 4) are within the pulse of activity that began around 600 ka in Costa Rica, but skewed to the younger side of the range.

[26] Because the bases of the active Nicaraguan volcanoes are covered by sediments, we cannot locate and sample the contact with older volcanics that would provide both age control and volume control. We can calculate reasonably precise volume measurements of the active volcanoes, using the surrounding plain as the base level. We then estimate an extrusive volcanic flux using the age of the oldest Nicaraguan lava sampled to date, 330 ka. This approach gives extrusive volume fluxes (in units of $km^3/km/Myr$) for western Nicaragua (4.7) and eastern Nicaragua (6.9) that bracket the volume flux for the Cordillera de Guanacaste (5.3) and are slightly less than the flux for the Cordillera
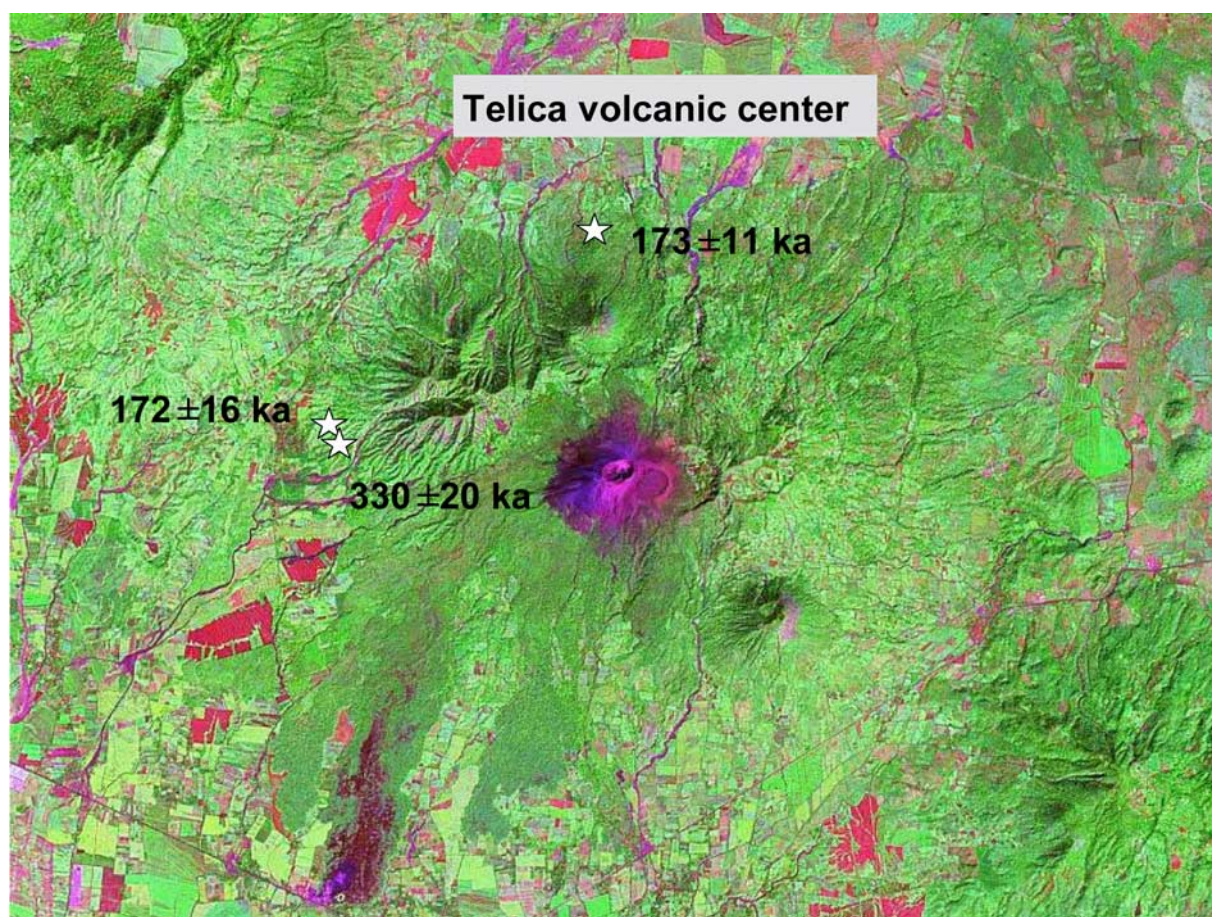
Figure 7. Satellite image of Telica volcano, Nicaragua, from NASA MrSID image N-16-10_2000.

Central (8.5). We expect that further efforts in geochronology will discover lavas somewhat older than the oldest current sample but expect that the oldest lavas will not be recovered except by drilling. We estimate the error in age as half the difference between the 600 ka datum from Costa Rica and the age of our oldest current sample. This gives an error estimate of 40%. The resulting extrusive volcanic flux errors for the two Nicaraguan segments are larger than those of the Costa Rican segments, even though the errors in the Nicaraguan volumes are lower.

[27] We test the reasonableness of the extrusive volcanic flux rates for Nicaragua by assuming a 600 ka date for the beginning of current cone construction and adding volume to the cones based on the depth to the pre-volcanic surface, following the estimates of *van Wyk de Vries* [1993]. Two arguments indicate that the depth to the base of the current volcanoes is not great. The first is a drill hole at the geothermal field on Momotombo volcano that intersected a dacitic ash flow, thought to

be the top to the Tertiary volcanics, at a depth of only 150 m below the present surface [*van Wyk de Vries*, 1993]. The second argument is the presence, within 15 km NE of the current volcanic front, of volcanic remnants whose ages are the same as the Monteverde volcanic front. Similarly, in the Nicaraguan Depression between San Cristóbal and Cosigüina volcanoes, there are low hills made of Tertiary volcanics, so that the depth of cover there is zero. Therefore we agree with *van Wyk de Vries* [1993] that the sediments that obscure the bases of the active volcanoes do not appear to be deep. We choose the drilling result at Momotombo volcano as the most reliable basis for estimating the depth to the bases of the volcanoes. We assume an interfingering relationship between the volcanic deposits and sediments, implying a cylindrical shape. We estimated the volumes representing the time between 600 ka and the current topographic base of the volcano by multiplying the area within the outer boundary of each volcano by 150 meters, the depth determined by drilling at Momotombo.

These assumptions add 176 km³ to the volumes of western Nicaraguan volcanoes and 212 km³ to the volumes of eastern Nicaraguan volcanoes. The resulting volume fluxes are 4.4 km³/km/Myr for western Nicaragua and 6.4 for eastern Nicaragua, slightly reduced from our preferred estimates in Table 2 but clearly consistent with them. To achieve the same flux rate for both the 330 ka datum and the 600 ka datum, the depth to the pre-volcanic surface needs to be increased by only 30 m.

3.3. Does the Extrusive Volcanic Flux Vary Along Nicaragua and Costa Rica?

[28] *Carr et al.* [1990] reported a paradoxical inverse correlation between degree of melting and volcano size in Central America. Degree of melting, inferred from rare earth element data, was high in Nicaragua and low in Costa Rica but the volumes of Nicaraguan volcanoes were small compared to Costa Rica. The recognition of a substantial late Pliocene to early Quaternary volcanic front in Costa Rica, the Monteverde VF, reduces the Costa Rican volumes and removes most of the disparity in size between Nicaragua and Costa Rica. The Nicaraguan magmas still appear to have formed from a higher degree of melting than the Costa Rican magmas but that difference may involve regional differences in the source of the magmas, specifically the general agreement now that the source in the Cordillera Central of Costa Rica is more enriched [e.g., *Malavassi*, 1991; *Herrstrom et al.*, 1995; *Feigenson et al.*, 2004].

[29] Although new geochronologic and geologic data have reduced the extrusive volcanic flux estimate for the Cordillera Central of Costa Rica, it remains larger than the flux estimates for the two Nicaraguan segments and the Cordillera de Guanacaste (Table 2 and Figure 8). However, the errors estimated for the calculation of extrusive volcanic flux (encompassing both volcano volume error and basal age uncertainties) are large enough to cover the remaining disparity. Thus the extrusive volcanic flux is considered constant along the volcanic front of Nicaragua and Costa Rica.

3.4. Average Compositions of Volcanic Centers and Groups

[30] Many studies have shown that two or more distinct magmas are sometimes present within the same volcanic center in Central America, even erupting from the same vent [e.g., *Ui*, 1972; *Walker*, 1984; *Reagan and Gill*, 1989; *Alvarado*
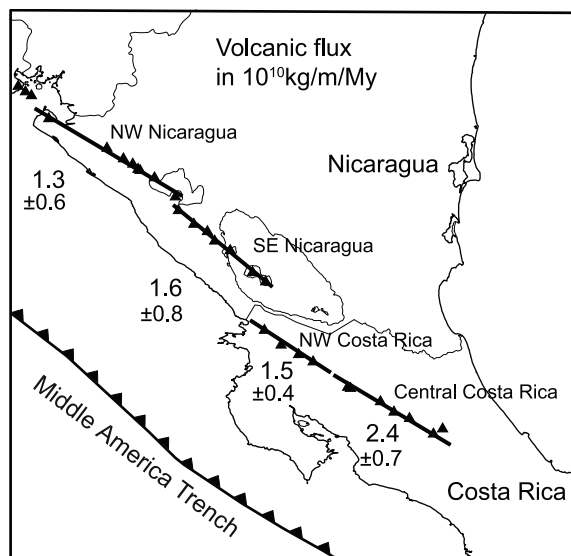

Figure 8. Extrusive volcanic flux by segment. The NW Costa Rica segment of the volcanic front includes the Cordillera de Guanacaste volcanoes. The central Costa Rica segment includes Arenal volcano and the Cordillera Central volcanoes.

and Carr, 1993; *Patino et al.*, 2000; *Carr et al.*, 2003; *Alvarado et al.*, 2006]. Therefore we decided to base our geochemical averages on individual volcanic centers and individual magma groups within a volcanic center. To calculate a flux for each center we made averages for each magma group at the center and then estimated the percentage of the total volume each group represented (Table 2). In most cases there was just one magma group. *Patino et al.* [2000] and *Plank et al.* [2002] took a simpler route and used average values for entire segments of the volcanic front.

[31] Although most of the samples used to determine average values were mafic, the resulting averages vary in SiO_2 and MgO content. To minimize any bias from this variation, we made a fractionation correction. Least squares fractional crystallization modeling of representative lava suites showed that a change of 1 wt% SiO_2 required 5% crystallization. We picked the least silicic average composition in each segment as the reference for that region and adjusted the other averages to it on the basis of the difference in SiO_2 contents.

3.5. Models of Mantle Sources

[32] The total flux of an incompatible element at an arc volcano consists of a mantle contribution and a
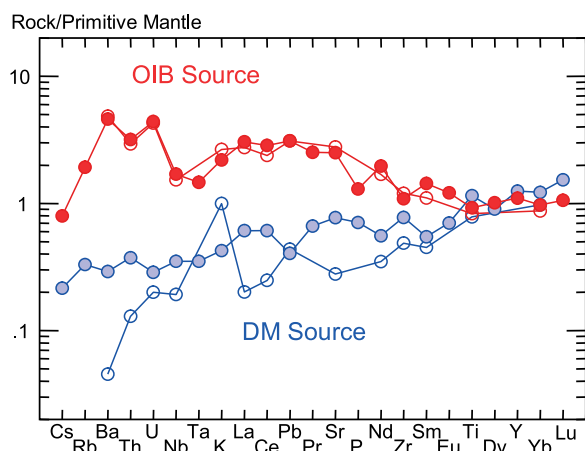
Figure 9. Sources for Central American volcanics. Open symbols from *Eiler et al.* [2005].

subducted contribution. Separating these two is not straightforward, because the mantle contribution is poorly constrained, both in its initial concentration and in the melting model to which it is subjected. *Patino et al.* [2000] estimated a source by inverting the EMORB values of *Sun and McDonough* [1989] using 15% batch melting. *Plank et al.* [2002] used the NMORB of *Sun and McDonough* [1989] divided by 3 as the mantle source. Neither of these studies concerned the Cordillera Central, where a more enriched source is present. *Eiler et al.* [2005] derived an enriched or OIB source by assuming that a Turrialba lava with minimal evidence of slab contribution was a 5% batch melt of a mantle composed of 51.6% olivine, 28.7% orthopyroxene, 16% clinopyroxene and 3.7% spinel. Because we examine a larger set of elements, we repeated that procedure using a similar lava (CR-IZ-D5) and the same mineral mode and extent of melting. Partition coefficients for missing REEs were interpolated from adjacent REEs. Rb partition coefficients were assumed equal to K, Cs equal to K/2, P equal to Sr and Ta equal to Nb. Despite these assumptions, our OIB source (Figure 9 and Table 3) is very similar to that of *Eiler et al.* [2005].

[33] The cleanest window into the unmodified Central American mantle comes from alkaline volcanoes, Utila and Yojoa, that erupted along faults generated by the Caribbean-North America plate boundary (Figure 1). At Yojoa, there are small Ba and Pb enrichments, consistent with O-isotope data indicating a minor slab contribution [*Eiler et al.*, 2005]. Therefore we chose Utila (Hon-UT-1) as the basis for DM. Employing the same mantle mode and partition coefficients used to derive the OIB source, we obtain DM, assuming that the Utila lava was the result of 0.5% batch melt. Because Hon-UT-1 lacks values for Nb, Ta and Pr, we estimated them by interpolation from adjacent elements on the spider diagram. The DM, derived from Utila, has about 10 times the Ba concentration as the DM of *Eiler et al.* [2005] (Figure 9). This seemingly radical difference has minimal effect on the subduction-derived Ba flux because the mantle contribution to Ba in Nicaragua, where this source is primarily used, is only 2 to 4% of the total. Using the lower Ba value from *Eiler et al.* [2005] would make the mantle contribution much smaller but only slightly increase the already large subduction-derived contribution.

3.6. Estimating Mantle Contributions

[34] We estimated the mantle contribution to the total incompatible element flux using mixtures of the two mantle sources and variable degrees of melting. For seven magma groups we had an initial model (Table 4), the source percentages and degrees of melting determined by *Eiler et al.* [2005]. With these models as starting points, we varied the proportions of the two mantle sources and the degrees of melting to fit the HREEs and the lowest elements on the spider diagrams, usually Nb and Ta. Examples of modeled mantle contributions are shown in Figures 10 and 11. Table 4 lists the mantle source percentages and the best fitting extents of melting for each group. The modeling also assumed the partition coefficients and mantle mode of *Eiler et al.* [2005] and batch melting.

Table 3. Composition of Mantle Sources

	Cs	Rb	Ba	Th	U	Nb	Ta	K_2O	La	Ce	Pb	Pr	Sr
DM	0.002	0.21	2.03	0.032	0.006	0.25	0.014	0.013	0.42	1.08	0.029	0.18	16.3
OIB	0.006	1.22	32.13	0.271	0.093	1.21	0.060	0.066	2.10	5.07	0.220	0.70	52.9

	P_2O_5	Nd	Zr	Sm	Eu	Gd	TiO_2	Tb	Dy	Y	Yb	Lu
DM	0.015	0.75	8.69	0.24	0.12	0.25	0.25	0.15	0.66	5.68	0.60	0.11
OIB	0.028	2.66	12.18	0.64	0.20	0.52	0.20	0.14	0.75	5.01	0.48	0.08

Table 4.   Models of Mantle Contribution

Volcanic Center or Group	Eiler et al. [2005]			Mantle Source		
	DM	OIB	Melt %	DM	OIB	Melt %
Cosigüina				100		15.0
San Cristóbal	95	5	15	100		10.0
Telica (high U/La group)	100		13	100		15.0
Telica (high Ba/Th group)				100		25.0
Telica (HFSE-rich group)				95	5	10.0
Rota				100		15.0
Las Pilas-Cerro Negro	100		25	100		20.0
Las Pilas (HFSE-rich group)				95	5	7.5
Momotombo and Apoyeque				100		15.0
Nejapa				100		25.0
Nejapa (HFSE-rich group)	100		12	95	5	10.0
Masaya				100		7.5
Mombacho and Zapatera				80	20	7.5
Granada (HFSE-rich group)	100		12	100		15.0
Concepcion				50	50	10.0
Maderas				50	50	10.0
Orosí				80	20	10.0
Rincón de la Vieja				80	20	10.0
Miravalles				80	20	7.5
Tenorio	80	20	7	80	20	15.0
Arenal				50	50	20.0
Platanar					100	10.0
Poás					100	10.0
Barba					100	10.0
Barba (HFSE-rich group)		100	6		100	4.5
Irazú-Sapper					100	10.0
Irazú-Haya (HFSE-rich group)		100	6		100	4.0
Turrialba					100	10.0

[35] Many of the magma groups listed in Tables 2 and 4 have very similar patterns on spider diagrams and effectively define clusters. In Nicaragua, the groups modeled with a pure DM source have nearly identical trace element patterns with the exception of Masaya, Granada and the Telica group with high Ba/Th. The peak in the regional Ba/La variation occurs in the western Nicaragua cluster (Figure 10a), which consists of seven groups that differ primarily in extent of melting, with a range from 10 to 25%. The mantle contribution model appropriate for the Cerro Negro-Las Pilas group, a 20% melt of DM, is included in Figure 10a. The spider diagram and the fitted mantle contribution model for Masaya (Figure 10c) suggests a lower extent of pure DM melting but this is likely an artifact. Masaya has a well-defined pattern of open-system magma evolution with at least two distinct inputs [Walker et al., 1993]. The increase in incompatible element contents at constant SiO₂ content caused by open system fractionation makes the HREE contents higher and our simple model sees that as a lower extent of melting. The Telica group with high Ba/Th cannot be closely fit using any combination of the two current mantle models. This misfit and similar problems for three of the HFSE-rich groups (discussed below) indicate that the OIB mantle is not be an appropriate enriched mantle source for western Nicaragua. The Granada HFSE-rich group has a notable lack of Nb and Ta depletion, no enrichment in K or Rb and moderate enrichments in Cs, Ba, U, Pb and Sr. The baseline is reasonably well fit as a 15% melt of DM.

[36] The groups that required an OIB component in the mantle source are shown in Figure 11. The groups with the poorest fits are the HFSE-rich groups from Telica, Las Pilas and Nejapa (Figure 11a). These groups differ from Granada by having enrichments in K and Rb. They differ from the other western Nicaragua groups by lacking Nb or Ta depletions and by having no suggestion of Zr or Ti depletions. The two Costa Rican clusters, Guanacaste and Cordillera Central are easily fit. This is not surprising given that the OIB source was derived from a lava from the Cordillera Central. The most plausible fit to the Concepción and Maderas cluster (Figure 10b) has a mantle source derived equally from DM and OIB.
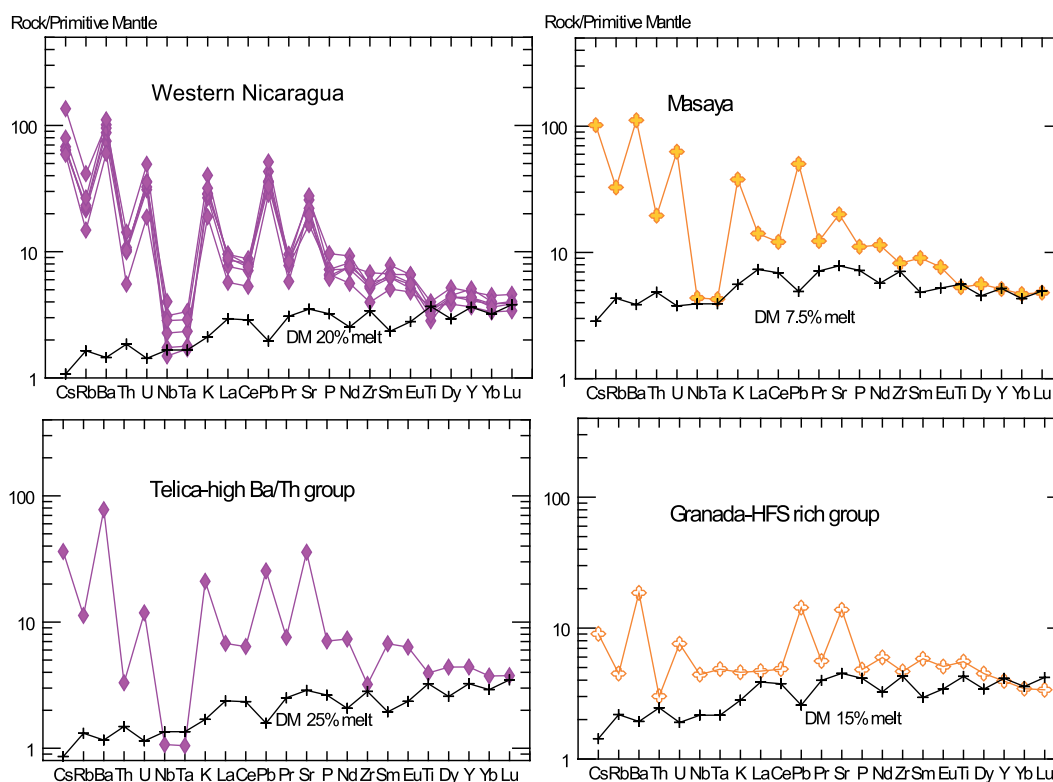
Figure 10. Spider diagrams of Nicaraguan volcanoes, whose modeled mantle-derived components are derived solely from DM. Selected models of mantle-derived component shown in black.

[37] The change in mantle source composition is not smooth along the volcanic front. The volcanic groups in Table 4 are ordered from NW to SE. In western Nicaragua the major source is DM but a more enriched source is likely always present but only revealed in low degree melts (HFSE-rich samples) that erupt before mixing into large magma chambers dominated by high degree melts. Proceeding southeast, the proportion of OIB source increases at Mombacho and then increases even more at Concepción and Maderas. The Guanacaste segment follows the large trenchward step in the volcanic front after Maderas and here the OIB component decreases. These results favor the complex intermingling of different sources in eastern Nicaragua and the Guanacaste proposed by *Reagan et al.* [1994] on the basis of U-series isotopes, rather than the abrupt transition at Tenorio volcano proposed by *Feigenson et al.* [2004] on the basis of Pb isotope variations.

[38] Our modeled mantle contributions primarily fit Nb and the HREEs, implicitly assuming that Nb, Ta and the heavy REEs are derived almost entirely from the mantle. For this assumption to hold, the fluids metasomatizing the mantle should have low

Nb contents or La/Nb of about 20. The high $\delta^{18}O$ slab phase of *Eiler et al.* [2005] has these characteristics but the low $\delta^{18}O$ slab phase has too much Nb. Most of the samples with low $\delta^{18}O$ are from Nicaragua and several of these are HFSE-rich lavas. The HFSE-rich lavas were not treated as a separate group and including them with the other Nicaraguan samples may have biased the calculated Nb for the low $\delta^{18}O$ phase. Furthermore, the Nb values available at that time were two to three times higher than our new data based on re-powdering the rocks.

3.7. Flux of Subducted Components From the Volcanic Front

[39] The contribution from the subducted slab is the difference between the modeled mantle contribution and the mean analysis. These values were adjusted for fractionation in a procedure that was the reverse of the fractionation correction described above. In this case, the mean SiO_2 that was adjusted to was not the mean for the relatively few analyses with high quality trace element data but the mean for the entire available major element suite, which is more representative of the volcano's
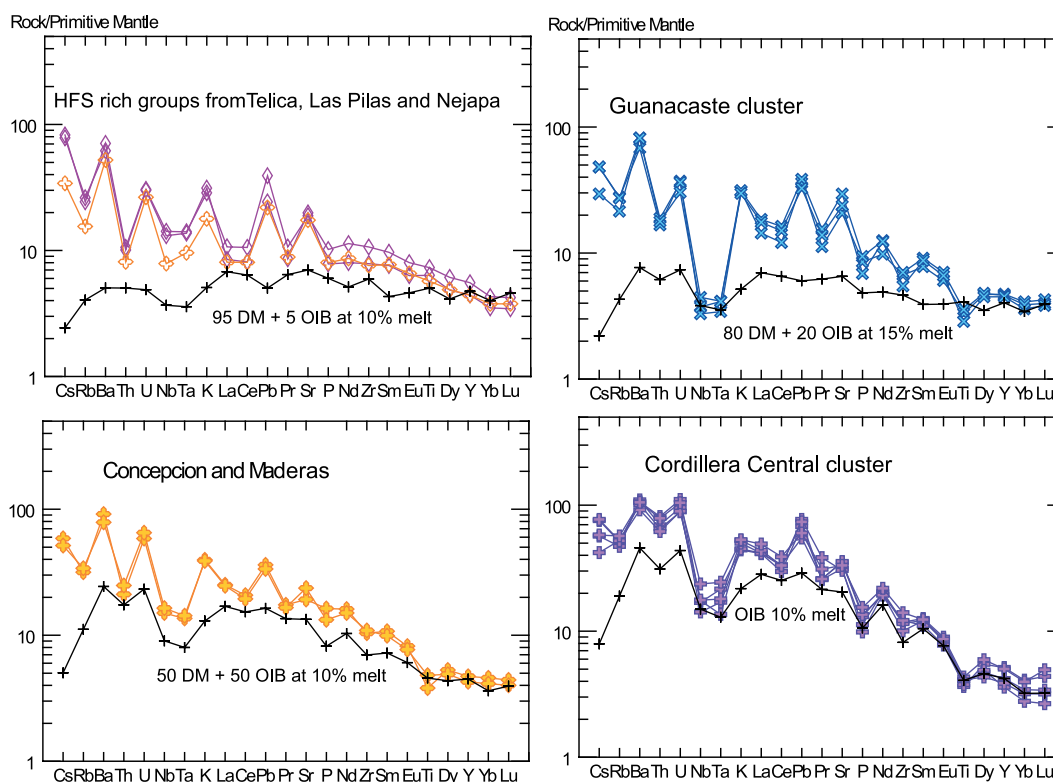
Figure 11. Spider diagrams of Nicaraguan and Costa Rican volcanoes, whose modeled mantle-derived components are derived from mixtures of DM and OIB or from pure OIB. Selected models of mantle-derived component shown in black.

actual composition. The fractionation corrected data were then multiplied by the mass flux, the last column of Table 2. The resulting subduction-derived element flux values are in the top section of Table 5. All of the compositions and calculations used are available in auxiliary material Table S1.

[40] The error involved in calculating a subduction-derived element concentration requires propagating errors from a large number of assumptions that are not easily quantified. Instead, we estimate percentage errors in concentration from the sensitivity of the subduction-derived element flux to assumptions about the mantle contribution. Our preferred subducted element fluxes are the top section of Table 5. We estimate maximum subduction-derived fluxes as the total fluxes (second section of Table 5). We define a first estimate of concentration error as one half of the difference between maximum flux and our preferred flux. We estimate a minimum subduction-derived flux by assuming that a line through the Th and Zr values on a spider diagram defines the mantle contribution. The values for the mantle component obtained this way are analogous to the Eu* parameter often used to define europium

enrichment or depletion on a REE plot. We did not extrapolate beyond Ba. We define a second estimate of concentration error as the differences between our preferred flux and the flux estimated relative to the Th-Zr line. We propagate the largest of these two concentration errors with the mass error to obtain a flux error.

[41] The concentration errors (Table 5) are large for the Cordillera Central, where the source is pure OIB. These errors may be caused, in part, by the awkwardness of our sensitivity approach. Nevertheless, we consider the subduction-derived element concentrations for the Cordillera Central poorly determined. Outside of the Cordillera Central, the concentration errors are small for the elements strongly enriched above the modeled mantle contribution (Cs, Rb, Ba, U, K, Pb). The errors for La, Th and, to a lesser extent, Sr are substantially larger.

[42] The errors in element flux, obtained by combining the mass flux errors (Table 2) and the largest of the two concentration errors, range from 24% to 155% of the totals for each element and each

Table 5. Fluxes and Error Estimates[a]

Segment (Mass Error)	Element								
	Cs	Rb	Ba	Th	U	K₂O	La	Pb	Sr
Subducted Element Flux									
NW Nicaragua	0.80	19.2	878	0.88	0.97	1.13	4.1	3.64	552
SE Nicaragua	1.04	25.0	1076	1.60	1.75	1.40	7.2	4.48	392
C. Guanacaste	0.73	27.4	892	1.75	1.14	1.42	9.6	3.55	554
C. Central	1.01	44.8	755	6.88	2.25	1.70	22.5	5.21	523
Total Flux (Maximum)									
NW Nicaragua	0.83	21.9	904	1.26	1.04	1.29	8.9	3.97	719
SE Nicaragua	1.09	32.2	1201	2.90	2.11	1.82	19.6	5.53	745
C. Guanacaste	0.78	34.3	1028	3.07	1.53	1.81	21.4	4.61	877
C. Central	1.24	89.1	1900	16.51	5.61	4.11	90.8	12.46	1948
Subducted Flux From Th-Zr (Minimum)									
NW Nicaragua			800	0.75	0.92	1.1	3.23	510	
SE Nicaragua			962	1.44	1.03	2.8	4.00	321	
C. Guanacaste			775	0.84	1.05	5.6	3.24	505	
C. Central			578	2.08	0.82	25.9	7.42	650	
*Concentration Error in % (Total Flux-Subducted Flux)/(2*Subducted Flux)*									
NW Nicaragua	1	7	1	22	4	7	58	5	15
SE Nicaragua	2	14	6	41	10	15	87	12	45
C. Guanacaste	3	13	8	38	17	14	61	15	29
C. Central	11	49	76	70	75	71	152	70	136
Concentration Error in % (ThZr Base-Subducted Flux)/(Subducted Flux)									
NW Nicaragua			9	23	19	73	11	8	
SE Nicaragua			11	18	26	61	11	18	
C. Guanacaste			13	26	26	42	9	9	
C. Central			23	8	52	−15	−43	−24	
Flux Error in % (Mass Error and Largest Concentration Error)									
NW Nicaragua (43%)	43	44	44	48	49	47	85	44	46
SE Nicaragua (50%)	50	52	51	65	53	57	100	51	64
C. Guanacaste (24%)	24	27	27	45	36	35	66	28	38
C. Central (31%)	33	58	82	77	81	77	155	76	140

[a] Fluxes in units of 10^4 kg/m/Myr, except K₂O, which is in units of 10^8 kg/m/Myr.

segment (bottom section of Table 5). These are generous errors because the inter-segment variations in subduction-derived flux are small for Cs, Ba, K and Pb and Sr (top section of Table 5). In fact, the standard deviations of the inter-segment variations for these elements are less than 20% of the means, substantially less than the estimated flux errors.

[43] If the regional variation in subduction signal, e.g., Ba/La (Figure 2), is the result of variations in flux, then the fluxes of highly enriched elements (top section of Table 5) should decrease from the NW Nicaragua segment to the Cordillera Central segment. Furthermore, the decrease should be substantial because Ba/La decreases by a factor of 10 across this region. However, the Ba fluxes do not decrease across the region and, in fact, do not

significantly change. Other highly enriched elements, whose fluxes show no regional variation, include Cs, K, Pb and Sr. What does change is the flux of Th and La, which increases from NW to SE. The La flux variation is roughly a factor of 5, similar to the range for Ba/La. However, the large errors estimated for the La and Th concentrations make us doubt that the regional variation in these modestly enriched elements is real. For these elements, a small decrease in extent of melting raises the mantle concentration and substantially reduces the subducted concentration. Alternatively, the southeastward increases in Th and La are real and reflect changes in the subduction component caused by additions of Galapagos derived volcanics that are highly enriched in incompatible elements. These inputs could be from seamounts or volcaniclastic sediments on the subducting slab

or from subduction erosion of the Costa Rican forearc [*Goss and Kay*, 2006].

4. Discussion

4.1. Magmatic Flux Versus Extrusive Volcanic Flux

[44] A bottom-up or long-term approach, applied to the Aleutian arc, yields an astonishingly high magma production rate of 110–205 km^3/km/Myr [*Jicha et al.*, 2006] or a slightly lower rate of 82 km^3/km/Myr [*Holbrook et al.*, 1999]. *Clift and Vannucchi* [2004] estimate a global magmatic arc productivity rate of 90 km^3/km/Myr, enough to replenish the crust they estimate is lost via subduction erosion. Their rate for Costa Rica, derived by adjusting the global rate to account for differences in the rates of plate convergence, is 108 km^3/km/Myr. In contrast, we estimate extrusive volcanic fluxes in Central America between 5 to 9 km^3/km/Myr, about a factor of 10 less than the means of various fluxes compiled by *White et al.* [2006]. However, most of the much higher flux estimates are total magmatic fluxes, averaged over very long time periods. Expanding the top-down approach, taken here, toward a total magmatic flux can begin with measurements of rates of erosion and volcaniclastic sedimentation. The mass of cumulates required to make the basaltic andesites and andesites most common at the volcanoes can be inferred from fractional crystallization modeling. Geophysics and structural geology may allow estimates of intrusive masses and a better determination of the depth to buried volcanic material along the active volcanic front in Nicaragua. The substantial gap between total magmatic flux and extrusive volcanic flux needs to be addressed.

4.2. Subduction-Derived Flux of Highly Enriched Elements

[45] Our primary result is that the fluxes of highly fluid mobile elements, Cs, Ba, K, Pb, and Sr are not significantly different along the Central American volcanic front from Nicaragua to Costa Rica. This constant flux is easy to reconcile with the similar rates of plate convergence and sediment thickness along the Middle America Trench. If the regional variation in slab signal (e.g., Ba/La in Figure 2) was caused by variation in the amount of a subduction-derived fluid, then the fluxes of Cs, Ba, K, Pb and Sr would be substantially greater for Nicaragua than for Costa Rica. This is not the case and the range of error in flux is small compared to the large variation in slab signal. Alternatively, there may be variations in subduction-derived fluids for the denominators in the slab signal ratios. La and Th flux would be substantially lower in Nicaragua than in Costa Rica. This is consistent with our estimates but the concentrations errors for La and Th are very large. The uncertainty in the Th and La fluxes could be substantially reduced by expanding our work to the northwestern half of the margin into El Salvador and Guatemala. The main difficulty with Th and La fluxes arises at the Cordillera Central segment in Costa Rica, where an OIB-rich source component, either in the mantle [*Feigenson et al.*, 2004] or from subduction [*Goss and Kay*, 2006], greatly complicates the problem of determining elemental fluxes. Present isotopic and trace element evidence shows that this complication is not present across El Salvador and into southeast Guatemala [*Carr et al.*, 2003].

[46] In Figure 2, the mantle contributions estimated from the parameters in Tables 3 and 4 are plotted as black crosses. Outside of the Cordillera Central in Costa Rica, the Ba contribution from the mantle is minimal and has little effect on the Ba/La ratio. La, however, is substantially derived from the mantle and the estimated mantle contributions overlap with the higher end of the range of 1/La values (Table 2b). This strengthens the argument that the Ba/La variation is derived primarily from La, whose concentration, in turn, varies with degree of melting and mantle wedge source composition.

[47] The chemical stratigraphy of the Cocos Plate sediments features an uppermost 100 meters of hemipelagic sediment that contains modest amounts of Ba but nearly all of the inventory of ^{10}Be and U [*Morris et al.*, 2002; *Patino et al.*, 2000]. The Ba flux will be modestly affected by sequestering part of this section but the ^{10}Be/^{9}Be signal will be greatly reduced. Therefore the regional variations in ^{10}Be/^{9}Be might be explained by differential subduction of the uppermost hemipelagic sediments. Subduction of the entire hemipelagic section offshore of Nicaragua and sequestering of the ^{10}Be-rich uppermost sediments offshore of Costa Rica are what is required. This possibility is well within the errors in our Ba and U flux estimates.

[48] Several weaknesses qualify our conclusion that the subduction-derived flux of highly fluid mobile elements is roughly constant along the margin. The first is the lack of any estimate of three prominent outputs from the volcanic front; the dispersed ashes, the eroded volcanics, making

their way to the Caribbean and the Pacific, and the masses of intrusives. However, it is unlikely that differences in these unmeasured parameters would be just the right size to greatly increase the flux in Nicaragua over Costa Rica. A second weakness is the appropriateness, or lack thereof, of the time frame we chose. We calculate the extrusive volcanic flux of the current generation of volcanoes. This approach includes an assumption that there are different generations of volcanics, that volcanic activity is episodic. Episodicity is the clear impression from field geology and it is the conclusion reached by detailed studies of Costa Rican geochronology and geology [*Alvarado et al.*, 1992; *Gillot et al.*, 1994; *Gans et al.*, 2003]. The larger problem is to measure the volcanic output over several volcanic pulses and calculate maximum, minimum and long-term rates. *Goss and Kay* [2006] estimated a long-term flux (over a 6 Myr period) for Pb and Th using the magmatic productivity rate of *Clift and Vannucchi* [2004]. Their fluxes are far higher than the ones we estimate because the magmatic productivity rate they start from is 15 times the volcanic flux we start from. The contrast between these two approaches makes clear that much work remains to be done.

[49] The largest geochemical problem is the appropriateness, or lack thereof, of the mantle-derived component of total flux. Following *Eiler et al.* [2005], we used one depleted and one enriched (OIB) mantle end-member, however the enriched component most likely varies along the arc. Away from Costa Rica, fits using OIB (estimated from a Cordillera Central lava) were generally poor. Good places to seek an enriched component, appropriate for Nicaragua, are the Granada and Nejapa volcanic lineaments in central Nicaragua. Volcanics from the back-arc, such as the alkaline cones near Pearl Lagoon on Nicaragua's Caribbean coast, are the best candidates for finding a clear window into the mantle beneath Nicaragua.

[50] We implicitly assumed that all elements are coursing through the system at the same rate and storage within the mantle wedge is not a factor. U-Series isotopes clearly show types of disequilibrium that suggest storage of some elements in the mantle wedge [*Reagan et al.*, 1994; *Thomas et al.*, 2002].

[51] We provide no constraint on the flux of water and so it may well vary along the lines proposed by *Ruepke et al.* [2002], *Ranero et al.* [2003], *Patino et al.* [2000], and *Abers et al.* [2003]. Water with a low inventory of highly incompatible elements, released from deep in the subducted plate, could

lead to a larger quantity of a more dilute fluid beneath Nicaragua. If so, then the water contents of Nicaraguan magmas should be higher. However, *Sadofsky et al.* [2005] presented melt inclusion results that argue for no change in the flux of water along the Central American margin.

5. Conclusions

[52] New geochronologic and geological data make a strong case for a 600 ka age for the beginning of the current volcanic front in Costa Rica. The primary change at that time was a near cessation of volcanic activity in the gap between the Cordillera de Guanacaste and the Cordillera Central. A basal age of 330 ka is suggested for the two volcanic segments in Nicaragua. This datum is not well established.

[53] The flux of extrusive volcanics along Nicaragua and Costa Rica varies between 1.3 and 2.4 × 10^{10} kg/m/Myr. These extrusive fluxes are about a factor of 10 lower than flux estimates published for other convergent margins, but most of these are total magmatic fluxes which are expected to be higher.

[54] Uncertainty over the trace element characteristics of the mantle beneath Central America make the calculated subduction-derived component of flux unreliable for elements that are only slightly or moderately enriched, such as Th and La. However, for Ba and other elements with very large enrichments over plausible unmodified mantle compositions, the uncertainly about the actual mantle composition becomes a relatively small factor in calculating the element flux.

[55] The subduction component of the fluxes of the highly fluid mobile elements Cs, Ba, K, Pb, and Sr are not significantly different along the Central American volcanic front from Nicaragua to Costa Rica.

Acknowledgments

References

Abers, G. A., T. Plank, and B. R. Hacker (2003), The wet Nicaraguan slab, *Geophys. Res. Lett.*, *30*(2), 1098, doi:10.1029/2002GL015649.

Alvarado, G. E., and M. J. Carr (1993), The Platanar-Aguas Zarcas volcanic centers, Costa Rica: Spatial-temporal association of Quaternary calc-alkaline and alkaline volcanism, *Bull. Volcanol.*, *55*, 443–453.

Alvarado, G. E., S. Kussmaul, S. Chiesa, P.-Y. Gillot, H. Appel, G. Wörner, and C. Rundle (1992), Resumen cronostratigráfico de las rocas ígneas de Costa Rica basado en dataciones radiométricas, *J. S. Am. Earth Sci.*, *6*, 151–168.

Alvarado, G. E., M. J. Carr, B. D. Turrin, C. C. Swisher, H.-U. Schmincke, and K. W. Hudnut (2006), Recent volcanic history of Irazú volcano, Costa Rica: Alternation and mixing of two magma batches, and pervasive mixing, in *Volcanic Hazards in Central America*, edited by W. I. Rose et al., *Spec. Pap. Geol. Soc. Am.*, *412*, 259–276, doi:10.1130/2006.2412(14).

Bolge, L. L., M. J. Carr, M. D. Feigenson, and G. A. Alvarado (2006), Geochemical stratigraphy and magmatic evolution at Arenal Volcano, Costa Rica, *J. Volcanol. Geotherm. Res.*, *157*, 34–48, doi:10.1016/j.jvolgeores.2006.03.036.

Carr, M. J., and W. I. Rose Jr. (1987), CENTAM-a data base of analyses of Central American volcanic rocks, *J. Volcanol. Geotherm. Res.*, *33*, 239–240.

Carr, M. J., M. D. Feigenson, and E. A. Bennett (1990), Incompatible element and isotopic evidence for tectonic control of source mixing and melt extraction along the Central American arc, *Contrib. Mineral. Petrol.*, *105*, 369–380.

Carr, M. J., M. D. Feigenson, L. C. Patino, and J. A. Walker (2003), Volcanism and geochemistry in Central America: Progress and problems, in *Inside the Subduction Factory, Geophys. Monogr. Ser.*, vol. 138, edited by J. Eiler and G. Abers, pp. 153–179, AGU, Washington, D. C.

Clift, P., and P. Vannucchi (2004), Controls on tectonic accretion versus erosion in subduction zones: Implications for the origin and recycling of the continental crust, *Rev. Geophys.*, *42*, RG2001, doi:10.1029/2003RG000127.

Deino, A., L. Tauxe, M. Monaghan, and A. Hill (2002), $^{40}Ar/^{39}Ar$ geochronology and paleomagnetic stratigraphy of the Lukeino and lower Chemeron Formations at Tabarin and Kapcheberek, Tugen Hills, Kenya, *J. Human Evol.*, *42*, 117–140.

Ehrenborg, J. (1996), A new stratigraphy for the Tertiary volcanic rocks of the Nicaraguan highland, *Geol. Soc. Am. Bull.*, *108*, 830–842.

Eiler, J. M., M. J. Carr, M. Reagan, and E. Stolper (2005), Oxygen isotope constraints on the sources of Central American arc lavas, *Geochem. Geophys. Geosyst.*, *6*, Q07007, doi:10.1029/2004GC000804.

Feigenson, M. D., and M. J. Carr (1993), The source of Central American lavas: Inferences from geochemical inverse modeling, *Contrib. Mineral. Petrol.*, *113*, 226–235.

Feigenson, M. D., M. J. Carr, S. V. Maharaj, S. Juliano, and L. L. Bolge (2004), Lead isotope composition of Central American volcanoes: Influence of the Galapagos plume, *Geochem. Geophys. Geosyst.*, *5*, Q06001, doi:10.1029/2003GC000621.

Gans, P. B., I. MacMillan, G. Alvarado-Induni, W. Pérez, and C. Sigarán (2002), Neogene evolution of the Costa Rican arc, *Geol. Soc. Am. Abstr. Programs*, *34*(6), 513.

Gans, P. B., G. Alvarado-Induni, W. Peréz, I. MacMillan, and A. Calvert (2003), Neogene evolution of the Costa Rican Arc and development of the Cordillera Central, *Geol. Soc. Am. Abstr. Programs*, *35*(4), 74.

Gillot, P. Y., S. Chiesa, and G. E. Alvarado (1994), Chronostratigraphy of upper Miocene-Quaternary volcanism in northern Costa Rica, *Rev. Geol. Am. Cent.*, *17*, 45–53.

Goss, A. R., and S. M. Kay (2006), Steep REE patterns and enriched Pb isotopes in southern Central American arc magmas: Evidence for forearc subduction erosion?, *Geochem. Geophys. Geosyst.*, *7*, Q05016, doi:10.1029/2005GC001163.

Herrstrom, E. A., M. K. Reagan, and J. D. Morris (1995), Variations in lava composition associated-with flow of asthenosphere beneath southern Central America, *Geology*, *23*, 617–620.

Herzberg, C. T., W. S. Fyfe, and M. J. Carr (1983), Density constraints on the formation of the continental Moho and crust, *Contrib. Mineral. Petrol.*, *54*, 1–5.

Holbrook, W. S., D. Lizarralde, S. McGeary, N. Bangs, and J. Diebold (1999), Structure and composition of the Aleutian island arc and implications for continental crustal growth, *Geology*, *27*, 31–34.

Jicha, B. J., Scholl, D. W. Singer, B. S. Yogodzinski, and S. M. Kay (2006), Revised age of Aleutian Island Arc formation implies high rate of magma production, *Geology*, *34*(8), 661–664, doi:10.1130/G22433.1.

Krushensky, R. D. (1972), Geology of Irazú Quadrangle, *U.S. Geol. Surv. Bull.*, *1353*, 46 pp.

Ledbetter, M. T. (1985), Tephrochronology of marine tephra adjacent to Central America, *Geol. Soc. Am. Bull.*, *96*, 77–82.

Leeman, W. P., M. J. Carr, and J. D. Morris (1994), Boron geochemistry of the Central American arc: Constraints on the genesis of subduction-related magmas, *Geochim. Cosmochim. Acta*, *58*, 149–168.

Malavassi, E. (1991), Magma sources and crustal processes at the southern terminus of the Central American volcanic front, Ph.D. thesis, 435 pp., Univ. of Calif. Santa Cruz, Santa Cruz.

Morris, J. D., W. P. Leeman, and F. Tera (1990), The subducted component in island arc lavas: Constraints from B-Be isotopes and Be systematics, *Nature*, *344*(6261), 31–36.

Morris, J., R. Valentine, and T. Harrison (2002), ^{10}Be imaging of sediment accretion and subduction along the northeast Japan and Costa Rica convergent margins, *Geology*, *30*(1), 59–62.

Patino, L. C., M. J. Carr, and M. D. Feigenson (2000), Local and regional variations in Central American arc lavas controlled by variations in subducted sediment input, *Contrib. Mineral. Petrol.*, *138*, 265–283.

Pérez, W., G. E. Alvarado, and P. B. Gans (2006), The 322 ka Tiribí Tuff: Stratigraphy, geochronology and mechanisms of deposition of the largest and most recent ignimbrite in the Valle Central, Costa Rica, *Bull. Volcanol*, doi:10.1007/s00445-006-0053-x.

Plank, T., and C. H. Langmuir (1993), Tracing trace elements from sediment input to volcanic output at subduction zones, *Nature*, *362*, 739–743.

Plank, T., V. Balzer, and M. J. Carr (2002), Nicaraguan volcanoes record paleoceanographic changes accompanying closure of the Panama Gateway, *Geology*, *30*, 1087–1090.

Ranero, C., and R. von Huene (2000), Subduction erosion along the Middle America convergent margin, *Nature*, *404*, 748–752.

Ranero, C. R., J. Phipps Morgan, K. McIntosh, and C. Reichert (2003), Bending-related faulting and mantle serpentinization at the Middle America trench, *Nature*, *425*, 367–373.

Reagan, M. K., and J. B. Gill (1989), Coexisting calcalkaline and high-niobium basalts from Turrialba Volcano, Costa Rica: Implications for residual titanates in arc magma sources, *J. Geophys. Res.*, *94*(B4), 4619–4633.

Reagan, M. K., J. D. Morris, E. A. Herrstrom, and M. T. Murrell (1994), Uranium series and beryllium isotope evidence for an extended history of subduction modification of the mantle below Nicaragua, *Geochim. Cosmochim. Acta*, *58*, 4199–4212.

Ruepke, L. H., J. Phipps Morgan, M. Hort, and J. A. D. Connolly (2002), Are the regional variations in Central American arc lavas due to differing basaltic versus peridotitic slab sources of fluids?, *Geology*, *30*−*11*, 1035−1038.

Sadofsky, S., K. Hoernle, and P. van den Bogaard (2005), Volatile cycling through the Central American volcanic arc from melt inclusion studies of Nicaraguan and Costa Rican magmas, in *Abstracts of the 15th Annual V. M. Goldschmidt Conference*, *Geochim. Cosmochim. Acta*, *69*(10), suppl., 663.

Stoiber, R. E., and M. J. Carr (1973), Quaternary volcanic and tectonic segmentation of Central America, *Bull. Volcanol.*, *37*, 304−325.

Sun, S., and W. F. McDonough (1989), Chemical and isotopic systematics of oceanic basalts: Implications for mantle composition and processes, in *Magmatism in the Ocean Basins*, edited by A. D. Saunders and M. J. Norry, *Geol. Soc. Spec. Publ.*, *42*, 313−345.

Thomas, R. B., M. M. Hirschmann, H. Cheng, M. K. Reagan, and R. L. Edwards (2002), $^{231}Pa/^{235}U$-$^{230}Th/^{238}U$ of young mafic volcanic rocks from Nicaragua and Costa Rica and the influence of flux melting on U-series systematics of arc lavas, *Geochim. Cosmochim. Acta*, *66*(24), 4287−4309.

Tournon, J., and G. E. Alvarado (1997), Mapa geológico de Costa Rica: Folleto explicativo, 80 pp. + geological map of Costa Rica, scale 1:500,000, Ed. Tecnol. de Costa Rica, Cartago.

Ui, T. (1972), Recent volcanism in the Masaya-Granada area, Nicaragua, *Bull. Volcanol.*, *36*, 174−190.

Vannucchi, P., D. W. Scholl, M. Meschede, and K. McDougall-Reid (2001), Tectonic erosion and consequent collapse of the Pacific margin of Costa Rica: Combined implications from ODP Leg 170, seismic offshore data, and regional geology of the Nicoya Peninsula, *Tectonics*, *20*−*5*, 649−668.

van Wyk de Vries, B. (1993), Tectonics and magma evolution of Nicaraguan volcanic systems, Ph.D. thesis, 328 pp., Open Univ., Milton Keynes, UK.

Villegas, A. (2004), La Formación Alto Palomo: Flujos pumíticos de le Cordillera Volcánica Central, Costa Rica, *Rev. Geol. Am. Cent.*, *30*, 73−81.

Vogel, T. A., L. C. Patino, G. E. Alvarado, and P. B. Gans (2004), Silicic ignimbrites within the Costa Rican volcanic front: Evidence for the formation of continental crust, *Earth Planet. Sci. Lett.*, *226*, 149−159.

von Huene, R., and D. W. Scholl (1991), Observations at convergent margins concerning sediment subduction, subduction erosion, and the growth of continental crust, *Rev. Geophys.*, *29*, 279−316.

von Huene, R., C. R. Ranero, W. Weinrebe, and K. Hinz (2000), Quaternary convergent margin tectonics of Costa Rica: Segmentation of the Cocos Plate, and Central American volcanism, *Tectonics*, *19*, 314−334.

Walker, J. A. (1984), Volcanic rocks from the Nejapa and Granada cinder cone alignments, Nicaragua, *J. Petrol.*, *25*, 299−342.

Walker, J. A., S. N. Williams, R. I. Kalamarides, and M. D. Feigenson (1993), Shallow open-system evolution of basaltic magma beneath a subduction zone volcano: The Masaya Caldera Complex, Nicaragua, *J. Volcanol. Geotherm. Res.*, *56*, 379−400.

White, S. M., J. A. Crisp, and F. J. Spera (2006), Long-term volumetric eruption rates and magma budgets, *Geochem. Geophys. Geosyst.*, *7*, Q03010, doi:10.1029/2005GC001002.